

# Machine Learning Classification and Regression Models for Predicting Directional Changes Trend Reversal in FX Markets

Adesola Adegboye<sup>a</sup>, Michael Kampouridis<sup>b,\*</sup>

<sup>a</sup>*School of Computing, University of Kent, Medway, ME4 4AG, UK  
Email: atna3@kent.ac.uk*

<sup>b</sup>*Centre for Computational Finance and Economic Agents,  
School of Computer Science and Electronic Engineering,  
University of Essex, Wivenhoe Park, CO4 3SQ, UK  
Email: mkampo@essex.ac.uk*

---

## Abstract

Most forecasting algorithms in financial markets use physical time for studying price movements, making the flow of time discontinuous. The use of physical time scale can make traders oblivious to significant activities in the market, which poses a risk. Directional changes (DC) is an alternative approach that uses event-based time to sample data. In this work, we propose a novel DC-based framework, which uses machine learning algorithms to predict when a trend will reverse. This allows traders to be in a position to take an action before this happens and thus increase their profitability. We combine our approach with a novel DC-based trading strategy and perform an in-depth investigation, by applying it to 10-minute data from 20 foreign exchange markets over a 10-month period. The total number of tested datasets is 1,000, which allows us to argue that our results can be generalised and are widely applicable. We compare our results to ten benchmarks (both DC and non-DC based, such as technical analysis and buy-and-hold). Our findings show that our proposed approach is able to return a significantly higher profit, as well as reduced risk, and statistically outperform the other trading strategies in a number of different performance metrics.

*Keywords:* Directional changes, Regression, Classification, Genetic programming, Forex/FX, Machine learning

---

## 1. Introduction

Financial forecasting is a major activity in financial markets. A big challenge faced by financial traders is the ability to identify security and market trends and so that they can maximise trading returns with minimal associated risk. An enormous amount of research has been dedicated to this topic (Brabazon et al., 2020), but it has been acknowledged from early on that financial time series are among the ‘noisiest’ and most difficult signals to forecast (Abu-Mostafa and Atiya, 1996). As a result, both the financial (and more recently the machine learning) literature has been continuously looking for new techniques that can lead to better trading results.

---

\*Corresponding author  
Email address: mkampo@essex.ac.uk (Michael Kampouridis)

8 The traditional approach used by financial traders is technical analysis. In this approach, traders use mathematical  
9 calculations in identifying and predicting repeating trends in historic data sampled in predetermined physical-time  
10 interval (Lin et al., 2017; Samanta et al.). An alternative approach to physical time data sampling is intrinsic time data  
11 sampling. In intrinsic series, data is sampled when events considered to be significant occur in the market (Cavalcante  
12 et al., 2016; Wan et al., 2016). The idea is that by focusing on important market activities, noise is obfuscated enabling  
13 traders build trading strategies around important trends. Over the years, different intrinsic time sampling techniques  
14 have emerged, such as perceptual important points (Chen and Chen, 2016; Chung et al., 2001), turning point (Yin  
15 et al., 2011), zigzag (Azzini et al., 2010; Özorhan et al., 2018), and directional changes (DC) (Glattfelder et al., 2011;  
16 Tsang, 2010; Tsang et al., 2017).

17 Directional Changes is a relatively new technique, and it has already demonstrated that it can yield profitable  
18 returns that can outperform state-of-the-art techniques, such as technical analysis indicators (Kampouridis and Otero,  
19 2017; Aloud, 2016). DC is based on the idea that an event-based system can capture significant points in price move-  
20 ments that the traditional physical time methods ignore. Hence, instead of looking at the market from an interval-based  
21 perspective, DC record the key events in the market (e.g., changes in the stock price by a pre-specified percentage)  
22 and summarise the data based on these events, moving away from a physical-time view to an event-based-time view.  
23 Under this new paradigm, a threshold  $\theta$  is defined, usually expressed by a percentage of the price. The market is then  
24 fragmented and summarised into upward and downward trends. Each of these trends are further dismembered into a  
25 directional change (DC) event and an overshoot (OS) event. Different thresholds produce different price summaries.  
26 Thus, the directional changes paradigm focuses on the size of price change, while time is the varying factor; whereas  
27 in the physical-time paradigm, time was fixed (e.g. daily closing prices).

28 In a previous work (Adegboye et al., 2017), we used a genetic programming (GP) algorithm to undertake symbolic  
29 regression and evolve equations that express linear and non-linear relationships between the length of DC and OS  
30 events in a given dataset. The advantage of that approach was that it allowed us to predict when a trend will reverse,  
31 and thus increase trading profitability. We used this approach as part of a DC-based trading strategy and tested it  
32 over 5 different Forex currency pairs for a total of 250 monthly datasets (5 DC thresholds, over 5 Forex pairs, over  
33 10 months). Our findings showed that our proposed approach was able to outperform other state-of-the-art trading  
34 approaches, such as a machine learning algorithm combining a number of technical indicators. This was a major  
35 finding, as it was one of the first works to demonstrate the competitiveness of our DC-based trading algorithms  
36 against state-of-the-art technical analysis indicators. This has also further motivated us to look for new and better  
37 ways to take advantage of the DC framework, as this could lead to improved profitability results.

38 This work poses an important step forward for more accurate trend reversal prediction, which as we mentioned  
39 earlier allows a trader to increase their profitability by being able to anticipate when the current trend will end. The  
40 main contribution of this paper is that we do not assume that a DC event is always followed by an OS event, as is often  
41 done in the literature. Instead, we create a new step, where we use a classification algorithm to predict whereas a DC  
42 event is going to be followed by an OS event. In the end, only when a DC event is classified having a corresponding

43 OS event, we go ahead with performing symbolic regression. This is an important contribution to our DC framework,  
44 as for certain datasets there can be a high number of DC events that are not followed by an OS event. Without this  
45 classification step, the symbolic regression GP tends to make conservative estimates of the OS length, as the GP builds  
46 equations even for DC events that do not have a corresponding OS event. The addition of the classification step in this  
47 work will allow the GP to focus only on DC events that are followed by an OS event, and thus lead to even better end  
48 of trend predictions than our previous work (Adegboye et al., 2017).

49 In addition to the above major contribution, this work also makes the following contributions: (i) We propose  
50 a new DC-based trading strategy that uses the combined classification and regression steps, (ii) We do not use the  
51 same set of fixed thresholds  $\theta$  across all datasets. Instead, we use a pool of thresholds and then the best thresholds (in  
52 terms of RMSE) are selected for each dataset. Thus, the thresholds we use are tailored to the datasets. (iii) We use a  
53 wide range of datasets from 20 Forex currency pairs. In total, our experiments are run over 1,000 different directional  
54 changes datasets, making our results much more significant and generalisable. (iv) We add seven new benchmarks and  
55 one more performance metric to enhance our results analysis. (v) We present samples of the best equations returned  
56 by the symbolic regression and discuss if we can have a generalised equation for predicting trend reversals across  
57 different datasets.

58 The above contributions will allow us to demonstrate not only the effectiveness of DC in terms of generating  
59 profitable trading strategies, but also its competitiveness against other state-of-the-art trading techniques. As explained  
60 at the beginning of this section, it is important to continuously look for new and improved techniques that lead to more  
61 profitable trading results. Our aim is thus to make a novel addition towards the goal of creating more profitable trading  
62 algorithms.

63 To achieve this aim, we have created the following objectives: (i) Demonstrate that the combination of classifica-  
64 tion and regression leads to error reduction when compared to other trend reversal algorithms, and (ii) Demonstrate  
65 that our proposed DC-based trading strategy, which utilises our proposed trend reversal approach, is able to be prof-  
66 itable and outperform other trading strategies, both DC and non-DC-based, including from physical time, such as  
67 technical analysis and buy-and-hold. More information about these aims will follow in Sections 3 and 5.

68 The rest of this paper is organized as follows: Section 2 provides an overview of the DC approach, as well as a  
69 discussion on the relevant literature. Section 3 presents all steps of our methodology, namely classification, regression,  
70 and trading strategy. Section 4 presents the experimental setup, and Section 5 presents and discusses our findings.  
71 Finally, Section 6 concludes the paper and discusses directions for future work.

## 72 **2. DC Background**

### 73 *2.1. Overview*

74 The directional change (DC) approach is an alternative approach for summarising market price movements. A  
75 DC event is identified by a change in the price of a given financial instrument. This change is defined by a threshold

76 value, which was in advance decided by the trader. Such an event can be either an upturn or a downturn event. After  
77 the confirmation of a DC event, an overshoot (OS) event usually follows. This OS event finishes once an opposite  
78 DC event takes place. The combination of a downturn event and a downward overshoot event represents a downward  
79 trend and, the combination of an upturn event and an upturn overshoot event represents an upturn trend. In other  
80 words, a downward trend is a period between a downturn event and the next upturn event and an upturn trend is a  
81 period between an upturn event and the next downturn event.

82 Figure 1 presents an example of how a physical-time price curve is transformed to the so-called *intrinsic time*  
83 (Guillaume et al., 1997) and dissected into DC and OS events. As we can observe, two different thresholds are used,  
84 and each threshold generates a different event series. Thus, each threshold produces a unique series of events. The  
85 idea behind the different thresholds is that each trader might consider different thresholds (price percentage changes)  
86 as significant. A smaller threshold captures a higher number of directional changes events, while a higher thresholds  
87 captures fewer directional changes events.

88 Looking at the events generated by a threshold of  $\theta = 0.01\%$  (events connected via red lines), we can observe that  
89 any price change less than this threshold is not considered a trend. On the other hand, when the price changes above  
90 that threshold, then the market is divided accordingly, to uptrends and downtrends. DC events are in solid lines, and  
91 OS events are in dashed lines. So a downturn DC event starts at Point A and lasts until Point B, when the downturn  
92 OS events starts. The downturn OS lasts until Point C, when there is a reverse in the trend, and an uptrend starts,  
93 which lasts until Point D. From Point D to E we are in an upturn OS event, and so on. The end/beginning price point  
94 of a new DC trend is called *DC Extreme point (DCE)*; these are Points A, C, E, and  $E'$ .

95 As we mentioned, different thresholds generate different event series. Looking at  $\theta = 0.018\%$  (events con-  
96 nected via dotted and dot-dashed lines), we can observe that the events generated are different: a downward trend  
97 starts from A and lasts until  $B'$ , and the downward OS is from Point  $B'$  until C. Then, from Point C until Point E there  
98 is an upward DC trend, and from E to  $E'$  there's an upward OS trend. Algorithm 1 presents the high-level pseudocode  
99 for generating directional changes events.

100 *It is important to note here that the confirmation of a change of a trend can only be confirmed retrospectively, i.e.*  
101 *only after the price has changed by the pre-specified DC threshold value  $\theta$ . For example, under  $\theta = 0.01\%$  we can*  
102 *only confirm that we are in a upward trend from Point D onwards. Point D is thus called a *DC Confirmation point**  
103 *(DCC). Before Point D, the directional change had not been confirmed (i.e. the market price had not changed by the*  
104 *pre-specified threshold value), thus a trader summarising the data by the DC paradigm would continue believing we*  
105 *are in a downward trend, which started from Point A. Similarly, a trader using  $\theta = 0.01\%$  would continue considering*  
106 *being in a upward trend from Point D until the price has reversed by  $\theta = 0.01\%$ , which only takes place at the next*  
107 *confirmation point, i.e., Point F. So what becomes important here is to be able to anticipate the change of the trend*  
108 *as early as possible, i.e. before Points C and E have been reached. In addition, since different thresholds generate*  
109 *different event series, we hypothesise that the combined information from these series would lead to profitable trading*  
110 *strategies.*

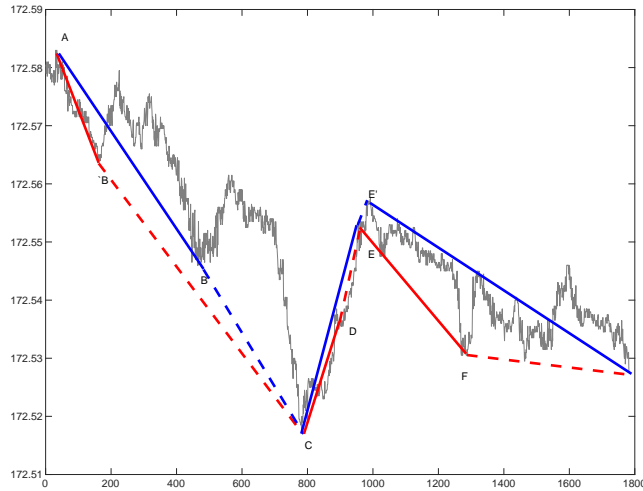


Figure 1: Directional changes for GBP/JPY currency pair. The red lines denote a set of events defined by a threshold  $\theta = 0.01\%$ , while the blue lines refer to events defined by a threshold  $\theta = 0.018\%$ . The solid lines indicate the DC events, and the dashed lines indicate the OS events. Under  $\theta = 0.01\%$ , the data is summarised as follows: Point  $A \mapsto B$  (Downward directional change), Point  $B \mapsto C$  (Downward overshoot event), Point  $C \mapsto D$  (Upward directional change), Point  $D \mapsto E$  (Upward overshoot event), Point  $E \mapsto F$  (Downward directional change). Under  $\theta = 0.018\%$ , the data is summarised as follows: Point  $A \mapsto B'$  (Downward directional change), Point  $B' \mapsto C$  (Downward overshoot event), Point  $C \mapsto E$  (Upward directional change), Point  $E \mapsto E'$  (Upward overshoot event). Points  $A, C, E,$  and  $E'$  are DCE points (DC Extreme). Points  $B, B', D, E,$  and  $F$  are called DCC points (DC Confirmation).

111 The advantage of this new way of summarising data is that it provides traders with new perspectives to price  
 112 movements, and allows them to focus on those key points that an important event took place, blurring out other price  
 113 details which could be considered irrelevant or even noise. Furthermore, DC have enabled researchers to discover new  
 114 regularities in markets, which are not captured by the interval-based summaries (Guillaume et al., 1997). Therefore,  
 115 these new regularities give rise to new opportunities for traders, and also open a whole new area for research.

---

**Algorithm 1** Pseudocode for generating directional changes events given threshold  $\Delta x_{dc}$ .

---

**Require:** Initialise variables (event is Upturn event,  $p^h = p^l = p(t_0)$ ,  $\Delta x_{dc}(Fixed) \geq 0$ ,  $t_0^{dc} = t_1^{dc} = t_0^{os} = t_1^{os} = t_0$  )

```
1: if event is Upturn Event then
2:   if  $p(t) \leq p^h \times (1 - \Delta x_{dc})$  then
3:     event  $\leftarrow$  Downturn Event
4:      $p^l \leftarrow p(t)$  //Price at end time for a Downturn Event
5:      $t_1^{dc} \leftarrow t$  //End time for a Downturn Event
6:      $t_0^{os} \leftarrow t + 1$  //Start time for a Downward Overshoot Event
7:   else
8:     if  $p^h < p(t)$  then
9:        $p^h \leftarrow p(t)$  //Price at start of Downturn event
10:       $t_0^{dc} \leftarrow t$  //Start time for Downturn event
11:       $t_1^{os} \leftarrow t - 1$  //End time for a Upturn Overshoot Event
12:    end if
13:  end if
14: else
15:   if  $p(t) \geq p^l \times (1 + \Delta x_{dc})$  then
16:     event  $\leftarrow$  Upturn Event
17:      $p^h \leftarrow p(t)$  //Price at end time for upturn event
18:      $t_1^{dc} \leftarrow t$  //End time for a Upturn Event
19:      $t_0^{os} \leftarrow t + 1$  //Start time for a Upturn Overshoot Event
20:   else
21:     if  $p^l > p(t)$  then
22:        $p^l \leftarrow p(t)$  //Price at start time for upturn event
23:        $t_0^{dc} \leftarrow t$  //Start time for a Upturn Event
24:        $t_1^{os} \leftarrow t - 1$  //End time for a Downturn Overshoot Event
25:     end if
26:   end if
27: end if
```

---

## 116 2.2. Related DC literature

117 An example of a regularity that has been discovered by using DC is the relationship between the DC event length  
118 and the OS event length (Glattfelder et al., 2011), where the OS length can be expressed as a function of the DC  
119 length. This insight can therefore be leveraged by traders for estimating a trend reversal, which is equal to the sum of  
120 the DC and OS event lengths, and as a result increase traders' profitability.

121 More specifically, Glattfelder et al. (2011) observed that the OS event length is on average twice the length of  
122 its preceding DC event (Equation 1). Kampouridis and Otero (2017) built on this work by treating the OS and DC  
123 length relationships as a linear function with a  $C$  constant, where  $C$  is the average DC length for a given dataset  
124 (Equation 2). Furthermore, because the above two works focused only on linear relationships, Adegboye et al. (2017)  
125 created a genetic programming (GP) algorithm to perform symbolic regression and generate both linear and non-linear  
126 relationships of DC and OS lengths (Equation 3). The advantage of this approach was that there were no assumptions  
127 for the relationship between DC and OS lengths, and it was up to the GP to uncover the function that describes this  
128 relationship.

$$OS_l \approx 2 \times DC_l \quad (1)$$

$$OS_l = C \times DC_l; C > 0 \quad (2)$$

$$OS_l = f(DC_l) \quad (3)$$

129 An interesting observation made in Adegboye et al. (2017), is that it is possible for a DC trend not to have a  
 130 corresponding OS event. In fact, we have observed that on certain datasets there can be as little as 14.77% of DC  
 131 trends with a corresponding OS event. This is, of course, threshold-dependent. Nevertheless, the fact remains that  
 132 one cannot assume that a DC event will always be followed by an OS event; it can be the case that a DC event is  
 133 followed by another DC event from the opposite direction. This was an important finding because it means that none  
 134 of the Equations 1-3 are taking this into account; as a result, the symbolic regression GP tends to make conservative  
 135 estimates of the OS length, as the GP builds equations even for DC events that do not have a corresponding OS event.

136 Thus, in this work, we introduce a classification task, which is going to predict whereas a DC event will have  
 137 a corresponding OS event. Only when this is true, we will be applying a GP algorithm to perform the symbolic  
 138 regression task and derive new formulas, based on Equation 3. The next section presents the classification step, along  
 139 with the other two steps of our methodology, namely regression and trading strategy.

### 140 3. Methodology

141 As explained in the previous section, there can be a high percentage of DC events that are not followed by an  
 142 OS event. Therefore, creating a symbolic GP algorithm to predict the length of an OS event as a function  $f$  of a DC  
 143 event (and thus predicting the end of the current trend) over the whole series of DC and OS events is an approach  
 144 with a major drawback: the resulted function  $f$  that describes this relationship does not take into account that many  
 145 DC events are not followed by an OS event. Hence a function in the form of  $OS_l = 2 \times DC_l$  would have been learnt by  
 146 using inaccurate data.

147 What we propose in our current work is to clearly separate the cases where a DC event is followed by an OS event  
 148 (we call this  $\alpha DC$ ), from those cases that a DC event is followed by another DC event of the opposite direction (e.g.  
 149 a downwards DC trend is directly followed by an upwards DC trend – we call this  $\beta DC$ ). In order to separate these  
 150 cases, we will be performing classification to predict whether a DC event is followed by an OS event. If the classifier  
 151 predicts that there will not be an OS event following the DC event, then there is no further action to be taken and  
 152 the trend reversal point will be the end of the DC event. On the other hand, if DC is followed by OS, then we will  
 153 use a symbolic regression model to represent the relationship between DC and OS lengths, and thus predict the trend  
 154 reversal point, which will be at the end of the OS event.

155 In order to achieve this, there is a number of steps that needs to take place. These steps are summarised in a swim  
 156 lane diagram in Figure 2. As we can observe, there is a number of operations taking place with the training dataset,  
 157 and these operations are then feeding into the test (unseen) dataset. More specifically, starting from the physical time  
 158 dataset (e.g. Forex prices at 10-minute intervals), we apply a GP algorithm, which will return three things: tailored DC  
 159 thresholds for the specific dataset (A), along with the generated DC dataset (C), and a model (formula) that describes

160 the relationship between DC and OS length (B). This process related to the symbolic regression GP will be described  
 161 in detail in Section 3.1. Then, AutoWeka is applied to the DC dataset to decide which is the optimal classification  
 162 algorithm for the given dataset. Then, the selected model is applied to the test (unseen) dataset, and will predict  
 163 whether a given DC event is followed by an OS event. Depending on the classification result, the algorithm has two  
 164 separate prediction points for the end of DC event; in the former case, it predicts that the trend will end at the end  
 165 of the OS event, whose length was estimated by the symbolic regression GP; in the latter case, since the classifier  
 166 has predicted that there is not going to be a corresponding OS event, the algorithm considers the end of the DC event  
 167 as the end of trend, and will thus take a trading action at that point. The above classification process is described in  
 168 further detail in Section 3.2. Lastly, the final step in our methodology is to use the predicted end of trend point as part  
 169 of a novel trading strategy, which is presented in Section 3.3.

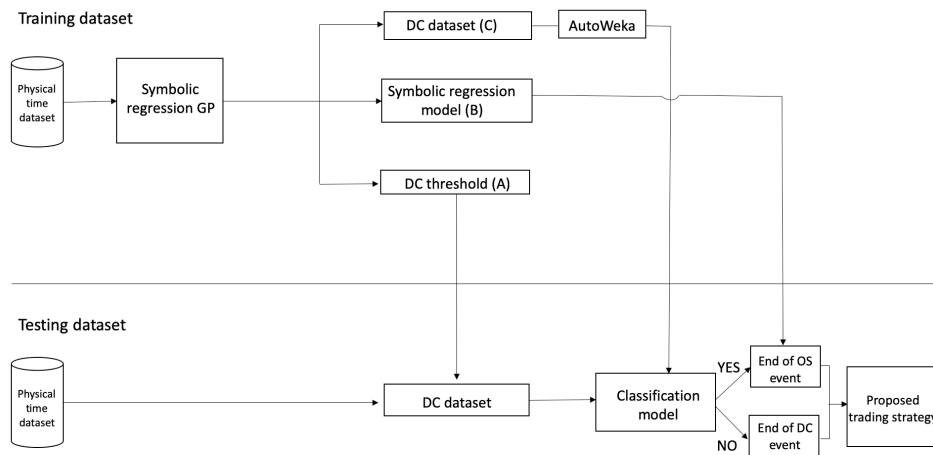


Figure 2: Our proposed methodology.

### 170 3.1. GP - Symbolic Regression

171 While standard regression techniques, such as linear regression, look for the optimal coefficient values (e.g.  $a, b$ )  
 172 for a given equation form (e.g.  $Y = aX + b$ ), symbolic regression allows us to determine both the functional form and  
 173 the appropriate coefficients. As a result, we do not need to make any assumptions about the relationship between the  
 174 given problem variables.

175 Genetic Programming is considered as state-of-the-art for symbolic regression tasks (Poli et al., 2008). Its ability  
 176 to build solutions (equations) without any assumptions of their form (i.e. GP is not constrained in building linear  
 177 equations, or even equations of a specific non-linear form), offers a unique advantage, as it allows it to determine  
 178 both the functional form of a given dataset, as well as its parameter values. It is based on the Darwinian principle of  
 179 evolution, where it creates a population of unfit (usually random) programs (equations describing the DC-OS length  
 180 relationship in our case), and searches the space of mathematical expressions to find linear and non-linear models



181 that best fit a given dataset. As our DC datasets are bivariate (DC and OS length), we are interested in finding a  
 182 mathematical equation that best describes the relationship between these two lengths.

183 Before going into details of the actual GP algorithm, it is important to clarify that even though the GP symbolic  
 184 regression model is inputted into our framework after the classification step (see Figure 2 above), in terms of imple-  
 185 mentation, it actually happens first. This is because if we perform the classification task first, then any classification  
 186 errors are going to affect the effectiveness of the GP models. More specifically, let us assume that we have a dataset  
 187 of 10 DC events, and that the first 8 DC events are followed by an OS event, whereas the last 2 DC events are not  
 188 followed by an OS event. Let us also assume that a classifier incorrectly predicts that all 10 DC events are followed  
 189 by an OS event. In this case, when we apply the GP to perform the symbolic regression task, it will be incorrectly  
 190 using information (data) from all 10 events in order to construct its models. But what would have been more accurate  
 191 would be applying the GP only to the DC events that have a corresponding OS event.

192 For this reason, we perform the GP regression task first under perfect foresight on the training dataset. So we  
 193 identify those DC events with a corresponding OS event and apply the GP to that data only. The advantage of this  
 194 approach is that we do not need to deal with the classification task and its corresponding classification errors. Instead,  
 195 we train the GP only on data that matters, instead of also including noise (i.e. DC events that are not followed with an  
 196 OS event). Furthermore, the fact that we only do this process on the training dataset avoids having any bias when we  
 197 eventually apply the selected GP model to the (unseen) test data.

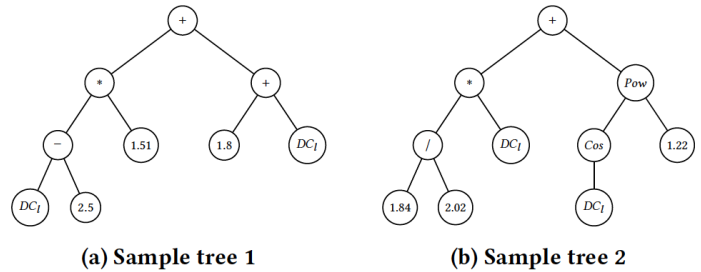


Figure 3: Sample GP individual trees: internal nodes are represented by arithmetic functions. The leaf nodes are represent by numeric constants and the DC length, denoted as  $DC_l$ . Given a DC event length the tree estimates the corresponding OS length.

### 198 3.1.1. Model representation

199 We represent our evolved GP individuals using tree structure. Every tree node has an operator function and every  
 200 terminal (a.k.a leaf) node has an operand, making mathematical expressions easy to evolve and evaluate. We utilise the  
 201 following 2-arity functions: addition, subtraction, division, multiplication, power and the following 1-arity functions:  
 202 sine, cosine, power, log, exponential. To prevent the GP from creating invalid solutions (e.g. division by zero), the  
 203 following functions are protected: division, logarithm, exponential and power. The terminal nodes consist of the DC  
 204 event length,  $DC_l$ , which is given as input, and also an ephemeral random constant (ERC), which is a no-argument

205 function that returns a random number. All functions and terminals are listed in Table 1.

206 Figure 3 presents two sample trees from our GP. The first tree represents the equation that calculates OS length as  
 207  $((DC_l - 2.5) \times 1.51) + (1.8 + DC_l)$  and the second trees represents the equation  $((\frac{1.84}{2.02}) \times DC_l) + (\cos(DC_l)^{1.22})$ , where  
 208  $DC_l$  in both equations is the length of DC event. As we can observe, the GP allows us to build both linear (Figure 3  
 209 (a)) and non-linear (Figure 3 (b)) relationships between DC and OS lengths. The trees are then going to be evaluated  
 210 against a given dataset and assigned an error, which indicates how well each tree (model) fits the data.

Table 1: GP Function and Terminal sets

Set	Value
Function set	addition, subtraction, division, multiplication, sine, cosine, power, log and exponential.
Terminal set	$DC_l$ , ERC.
Genetic operation	elitism, subtree mutation and subtree crossover

### 211 3.1.2. Model evaluation

212 It is important to highlight here that the confirmation of a change from upward DC trend to downward DC trend  
 213 and vice-versa can only be confirmed retrospectively after the price has changed by the pre-specified DC threshold  
 214 value. Once a directional change is confirmed and a DC trend is classified to be compose of both DC event and  
 215 OS event, traders are better informed on the potential point in time when DC trend is expected to reverse if OS  
 216 event length can be adequately estimated. This potential point in time will be the sum of DC event length known at  
 217 DCC (DC Confirmation point) and OS event length of the  $\alpha DC$  estimated using our GP model. To evaluate our GP  
 218 model we measure the error between actual OS length ( $OS_l$ ) and estimated OS length ( $\hat{OS}_l$ ). To describe our model  
 219 performance, we measure the error  $\varepsilon$  using RMSE shown in Equation 4.

$$\varepsilon = \sqrt{\frac{\sum_{i=1}^N (OS_l - \hat{OS}_l)^2}{n}} \quad (4)$$

220 where  $n$  is the sample size.

221 During evolution, we penalise trees that have only constants as terminal nodes, trees that estimate a negative value  
 222 and trees that evaluate fitness to NaN or infinity. We perform tournament selection and select parents based on fitness  
 223 level. We also consider tree depth as a secondary selection criteria in cases where the lowest RMSE is attained by  
 224 more than one tree. We give preference to the tree with a shorter depth.

### 225 3.1.3. Operators and other parameters

226 We use elitism, subtree mutation and subtree crossover (see Table 1). To control growth, we use hard limits on the  
 227 depth of offspring programs generated. *Maximum\_depth* is used for controlling mutation operation.

228 We have introduced a wrapper to replace incorrect predictions of  $OS_l$  with 0. This value was necessary because  
 229 it was possible for GP to predict negative, NaN or infinite OS length value. We chose the value of 0 because after  
 230 empirical observations, we realised that there were cases where a DC event is directly followed by another DC event  
 231 of the opposite direction, hence the OS length of the preceding DC event was 0.

#### 232 3.1.4. GP outputs

233 So far we have discussed using the GP to perform the regression task on DC-based data. However, a problem we  
 234 faced was which DC threshold to use. As we have already mentioned, different DC thresholds produce completely  
 235 different different DC event series. For example, as we showed in Figure 1, a 0.01% threshold produces different event  
 236 series to a 0.018% threshold.

237 In order to decide which thresholds to use during our experiments, we create a pool of DC thresholds. Each  
 238 threshold then generates a different DC event series. Then, we apply the GP to each one of these event series. As a  
 239 result we obtain a GP symbolic regression model for each DC event series. Lastly, we rank all GP models in terms of  
 240 RMSE. This allows us to obtain three outputs: the best GP model, its corresponding DC event series and threshold (  
 241 i.e. used in generating the corresponding event series). This process is summarised in Figure 4.

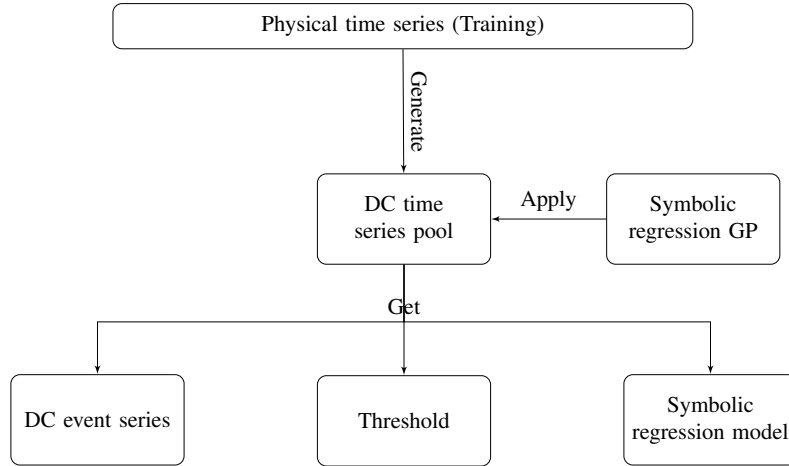


Figure 4: Our proposed framework for evolving symbolic regression model and selecting threshold and DC event with high DC:OS event ratio.

#### 242 3.2. Classification

243 The next step in our framework is to classify whereas a DC trend is composed by a DC event and an OS event  
 244 ( $\alpha DC$ ), or if a DC trend is solely composed of a DC event ( $\beta DC$ ). As there are numerous classification algorithms  
 245 that can be used for this task, we decided to use Auto-Weka (Thornton et al., 2013), a well-known automated machine  
 246 learning algorithm. While Weka (Frank et al., 2016), which is a well-known open source package, provides many  
 247 classification algorithms ready to be used off-the-shelf, there are two important decisions that need to be made: (i)  
 248 which algorithm to choose for the specific task, and (ii) what are the hyperparameter values for the selected algorithm.

249 Auto-Weka overcomes this problem, as it uses recent advances in high-dimensional stochastic optimisation to fully  
 250 automate the above processes. In the end, Auto-Weka returns the best performing algorithm (a classifier in our case),  
 251 along with an optimal selection of its hyperparameter values with minimal human intervention.

252 We apply Auto-Weka to each dataset, thus each dataset can end up using a different classification algorithm (Auto-  
 253 Weka has a choice of 39 classification algorithms). The advantage of this is that we have a tailored classification  
 254 algorithm and tailored hyperparameters *for each dataset*. To avoid any bias, Auto-Weka is only applied to the training  
 255 dataset and is trained using 10 k-fold cross-validation. In order to decide which classification model to use for each  
 256 dataset, we run Auto-Weka 10 independent times per dataset, and in the end we select the classification model with  
 257 the best f-measure.

258 The attributes used for the classification task are all DC-related and are presented in Table 2. As we can observe,  
 259 we use 6 different attributes, which are related to DC and OS events' price and time, as well as the speed of price  
 260 changing. Attributes X1, X2, were first derived and presented in Glattfelder et al. (2011). Furthermore, attributes X3,  
 261 X4, X5 and X6 were created for the purposes of this paper, after experimenting with a set of different attributes and  
 262 identifying the ones with the best classification performance on a training dataset.

Attributes	Name	Description
X1	DCevent price	This is the price difference between the up- turn/downturn point and the directional change confirmation point.
X2	DCevent time	This is the time difference between the up- turn/downturn point and the directional change confirmation point.
X3	$\sigma'$	This is the speed at which price change from the start of a trend to directional changes confirma- tion point.
X4	$DC_{event_{-1}}$ price	This is the market price at the previous confir- mation point.
X5	$DC_{event_{-1}}$ OS	This is a Boolean variable (Yes/No). Indicates whether the immediate previous DC trend has an OS event.
X6	Flash event	This is a Boolean variable (Yes/No). Indicates whether DC event start time and end time are equal.

Table 2: Classification attributes - A brief description of independent variables used for classifying whether a DC trend has OS event or not.

263 The classification process is summarised in Figure 5. As we can see, we use the 'Best DC event series' as input.  
 264 This is essentially one of the three outputs of the GP process presented in Figure 4 and detailed in Section 3.1. We thus

265 use this event series to create DC attributes for our classification task. Auto-Weka is then applied to these attributes  
 266 and at the end we obtain the best classification model for each dataset. A reminder that this whole process takes place  
 267 for the training data.

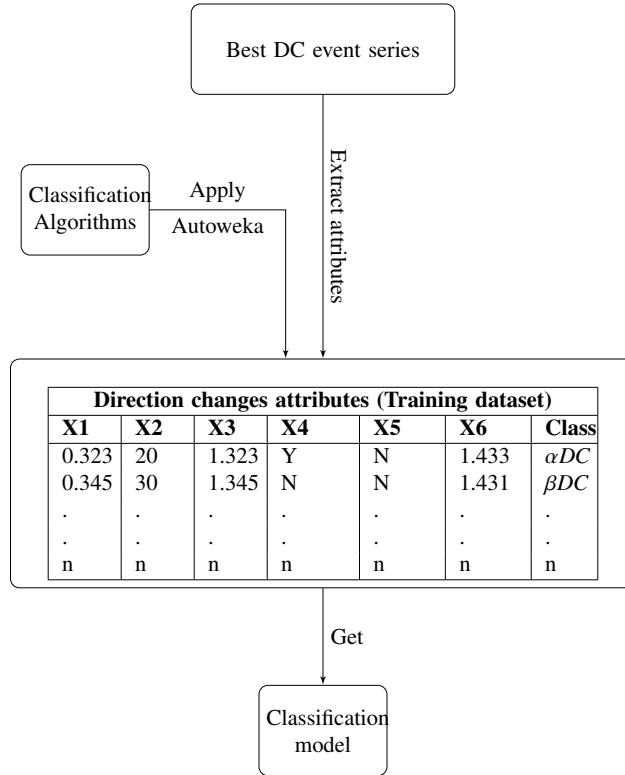


Figure 5: Our proposed framework for creating classification model. The classification model classifies DC trends into  $\alpha DC$  and  $\beta DC$

268 Once the classification process is also completed, we are then ready to predict the end of a trend in the (unseen)  
 269 test set by combining the outputs of the classification and the regression steps. What we therefore do is apply the  
 270 classification model obtained from the training data to the test dataset and classify whether a DC trend is composed  
 271 by both a DC and OS event ( $\alpha DC$ ), or not. If the answer is no, then we can predict that the end of the trend will be at  
 272 the end of the current DC event ( $DC_t$ ). On the other hand, if a DC event is followed by an OS event, then we can use  
 273 the symbolic regression model obtained in Section 3.1 and predict the trend reversal point, which is the sum of the  
 274 DC and OS lengths. This process was also illustrated earlier in Figure 2, which was presented earlier at the beginning  
 275 of Section 3.

### 276 3.3. Trading Strategy

277 The first two steps presented in the previous two sections allow us to predict the end of a trend in DC event series.  
 278 To understand how effective this prediction is, we need to use it as part of a trading strategy. In order to do this, we  
 279 embed our trend reversal prediction process into a trading strategy. For the remainder of this section, we present the  
 280 trading strategy we use in our experiments.

281 3.3.1. Trading strategy overview

282 In order to decide how to trade, we differentiate between opening and closing a position. Opening a position  
283 means we sell the base currency and buy the quoted currency. Closing a position means we buy the base currency and  
284 sell the quoted currency. We open a position at upward DC trends, provided there is not an existing open position and  
285 return is positive after deducting transaction costs. We close a position if there is an existing open position and return  
286 is positive after deducting transaction costs. In all other cases we adopt a hold trading strategy. All transactions are  
287 done using our entire capital. The transaction cost is 0.025% per transaction. The Opening and Closing strategies are  
288 summarised in Algorithms 2 and 3.

---

**Algorithm 2** Trading rules used for selling base currency

---

**Require:** Sell rule

**if** DC trend is upward **then**

**if** There is no open position **then**

**if** Is  $\beta DC$  && Return is not negative **then** Open a position at DCC point

**else if** Is  $\alpha DC$  && DC trend does not reverse before estimated DCE point && Return is not negative **then**

Open a position at estimated DCE point

**else** Hold

**end if**

**end if**

**end if**

---

---

**Algorithm 3** Trading rules used for buying base currency

---

**Require:** Buy rule

**if** DC trend is downward **then**

**if** There is an open position **then**

**if** Is  $\beta DC$  && Return is not negative **then** Close position at DCC point

**else if** Is  $\alpha DC$  && DC trend does not reverse before estimated DCE point && Return is not negative **then**

Close position at estimated DCE point

**else** Hold

**end if**

**end if**

**end if**

---

289 3.3.2. Trading strategy evaluation

290 To evaluate our trading strategy, we measure profitability and risk. We report return, mean maximum drawdown  
291 (MDD) and sharp ratio. Return, shown in Equation 5 is the accumulated profit or loss during our trading period and it  
292 is calculated by deducting transaction cost from quantity of Forex available for trading and multiplying the result with  
293 the exchange rate. Transaction cost shown in Equation 6 is the expense incurred for effecting a trade transaction, in  
294 our case the sale or purchase of a foreign currency and it is calculated as 0.025% of the quantity of Forex available for  
295 trading. MDD shown in Equation 7 is the downside risk of our strategy and it is measured by calculating the maximum  
296 observed loss from a peak price to a trough before a new peak is reached. To measure our excess return, above the

297 risk-free rate, we use Sharpe ratio shown in Equation 8. It measure the amount of risk involved in obtaining our  
 298 returns. It is calculated by deduction risk-free rate from mean return and dividing the result by the standard deviation.  
 299 In this work, we assign 0 as our risk-free rate.

$$R = (Q - TC) \times FXrate \quad (5)$$

$$TC = Q \times \frac{0.025}{100} \quad (6)$$

$$MDD = \frac{P_{trough} - P_{peak}}{P_{peak}} \quad (7)$$

$$SharpeRatio = \frac{R - RFR}{\sigma_R} \quad (8)$$

300 where  $R$  is the return,  $Q$  is the quantity,  $TC$  the transaction cost,  $FXrate$  the FX rate of the relevant currency pair,  
 301  $MDD$  is the Maximum Drawdown,  $P_{trough}$  the trough of the price,  $P_{peak}$  the peak of the price,  $RFR$  the risk free rate,  
 302 and  $\sigma_R$  is the standard deviation of the return.

#### 303 4. Experimental setup

304 This section is divided into the following parts: Section 4.1 presents the data we are using for the experiments,  
 305 Section 4.2 presents the tuning configurations for the classification and regression tasks of our framework, and lastly,  
 306 Section 4.3 presents the setup of the trading experiments.

##### 307 4.1. Data

308 We used 10-minute interval high frequency data from March 2016 to February 2017 of the following currency  
 309 pairs: AUD/JPY (Australian Dollar and Japanese Yen), AUD/NZD (Australian Dollar and New Zealand Dollar),  
 310 AUD/USD (Australian Dollar and US Dollar), CAD/JPY (CAD Dollar and Japanese Yen), EUR/AUD (Euro and  
 311 Australian Dollar), EUR/CAD (Euro and Canadian Dollar), EUR/CSK (Euro and Czechoslovak koruna), EUR/NOK  
 312 (Euro and NOK), GBP/AUD (British Pound and Australian Dollar), NZD/USD (New Zealand Dollar and US Dollar),  
 313 USD/CAD (US Dollar and Canadian Dollar), USD/NOK (US Dollar and Norwegian Krona), USD/JPY (US Dollar  
 314 and Japanese Yen), USD/SGD (US Dollar and Singaporean Dollar), USD/ZAR (US Dollar and South African Rand),  
 315 EUR/GBP (Euro and British Pound). We also used 10-minute interval data from June 2013 to May 2014 of the follow-  
 316 ing currency pairs: EUR/USD (Euro and US dollar), EUR/JPY (Euro and Japanese Yen), GBP/CHF (British Pound  
 317 and Swiss Franc), and GBP/USD (British Pound and US dollar). All data was purchased from OLSENDA.com.  
 318 We considered each month in the period as a separate physical-time dataset. In our tuning phase we used 200 DC

319 datasets for tuning (i.e. 5 thresholds  $\times$  20 currency pairs  $\times$  first 2 months of our physical-time data). For the rest of our  
 320 experiment we use 1000 DC dataset (i.e. 5 DC thresholds  $\times$  20 currency pairs  $\times$  remaining 10 months of our physical  
 321 time datasets). Our tuning and non-tuning DC dataset were split in 70:30 ratio as our training and testing sets.

322 As different DC thresholds produce different DC event series, we have chosen to evaluate 5 different thresholds for  
 323 all tuning and non-tuning DC datasets. These thresholds are the best 5 thresholds that are dynamically selected during  
 324 the GP regression step presented in Section 3.1. In the results section, we will be reporting the average performance  
 325 of each algorithm, over these 5 DC thresholds.

#### 326 4.2. Regression and classification algorithms' tuning

327 The only parameter of Auto-Weka that required tuning was its execution time. This is because Auto-WEKA  
 328 requires to be given enough time to search its algorithms and hyperparameter space for a classification model that is  
 329 best in predicting our two class labels ( $\alpha DC$ ,  $\beta DC$ ). We experimented with different runtime configurations namely  
 330 15 minutes, 30 minutes, 45 minutes 60 minutes, 75 minutes. We chose a runtime of 60 minutes based on average  
 331 f-measure, which we observed to diminish at a runtime of 75 minutes. Depending on the number of CPU cores  
 332 available, it is possible to execute Auto-Weka in serial or parallel mode. For our experiment we executed Auto-Weka  
 333 in serial mode, using 1 CPU core.

334 Genetic Programming algorithms have a number of parameters that require tuning, such as the number of the  
 335 individuals (population), the number of iterations where learning takes place learning (generations), the number of  
 336 individuals that compete to become a parent in the crossover and mutation operators (tournament size), the proba-  
 337 bility that we apply genetic operators to a given GP individual (crossover probability, mutation probability, elitism  
 338 probability), and the maximum depth that a GP tree is allowed to grow (maximum depth). We tuned the above pa-  
 339 rameters using the I/F-Race package(López-Ibáñez et al., 2011), which implements racing methods for the selection  
 340 of the best configuration for an optimisation algorithm by empirically selecting the most appropriate settings from a  
 341 set of instances of an optimisation problem(Birattari et al., 2010). Table 3 presents the values of the GP parameters as  
 342 determined by I/F-Race.

Parameter	
Population	500
Generation	37
Tournament size	3
Crossover probability	0.98
Mutation probability	0.02
Elitism probability	0.10
Maximum depth	3

Table 3: Regression GP experimental parameters for detecting DC-OS relationship, determined using I/F-Race.



343 *4.3. Trading experimental setup*

344 As we have already explained, after completing the classification and regression tasks, our framework can make a  
345 prediction on when a DC trend ends. We can then embed this as part of the trading strategy we presented in Section  
346 3.3. This is our proposed algorithm and is called it C+GP+TS.

347 In order to evaluate the efficiency of our proposed algorithm, we will be comparing it with several other bench-  
348 marks. Below we present in detail the different algorithms that we use to benchmark our approach. These benchmarks  
349 can be separated into two categories: DC-related algorithms, and non-DC-related algorithms.

350 *4.3.1. DC-related benchmarks*

351 **O+TS.** This is a DC trend reversal approach originally presented in Glattfelder et al. (2011), where it was observed  
352 that on average OS event length is twice the DC event length. In this trading strategy, instead of embedding our  
353 classification and regression steps, we embed Equation 1. Thus, the trend reversal point becomes the point where the  
354 OS event length is twice the DC length.

355 **M+TS.** This is a DC trend reversal approach originally presented in Kampouridis and Otero (2017), where a constant  
356 was used to describe the linear relationship between DC and OS length. This constant was tailored to each dataset and  
357 separate ratios were calculated for upward trends and downward trends. In this trading strategy, instead of embedding  
358 our classification and regression steps, we embed Equation 2. Thus, the trend reversal point is tailored to each dataset.

359 **GP+TS.** This is a DC trend reversal approach presented in Adegboye et al. (2017), where symbolic regression GP is  
360 used to evolve an equation which represents the ratio between DC event length and OS event length in a dataset. This  
361 is the predecessor of our proposed approach, as while it includes the regression step, it does not have the classification  
362 step. In this trading strategy, we embed Equation 3.

363 *4.3.2. Non-DC benchmarks*

364 **Technical analysis trading strategy.** Technical analysis trading strategies is a very popular approach in trading. It  
365 uses technical indicators, for insight into when to make trading decisions. We experimented with seven trading  
366 strategies that utilise the following indicators; Exponential Movement Average (EMA), Bollinger Bands (BOLLIN),  
367 Simple Moving Average (SMA), Aroon Oscillator (AROON), Rate of Change (ROC), Relative Strength Index (RSI)  
368 and Moving Average Convergence Divergence (MACD), respectively.

369 **Buy and hold.** Buy and hold is a well-known benchmark for trading algorithms. Under this trading strategy we  
370 bought the quoted currency in the first month of our non-tuning data, then sold it in exchange for the base currency  
371 after the 10 month period.

## 372 5. Result and analysis

373 This section presents results for our experiments. It is divided into three main sections: Section 5.1, which presents  
374 the classification results, Section 5.2, which presents the regression results, and Section 5.3, which presents the trading  
375 results.

376 We would like to one more time remind the reader that the theoretical contribution of the work are as follows:  
377 (i) provide empirical evidence that classification models are effective in detecting the existence of trends before they  
378 reverse, thus, providing traders with alternate signal to improve their decision making when trading, (ii) provide  
379 empirical evidence that symbolic regression GP models are successful at predicting the point in time when trend is  
380 expected to reversal given that the DC trend has an overshoot event, (iii) Demonstrate that by combing our classi-  
381 fication and symbolic regression models, prediction error can be considerably reduced when compared to other DC  
382 based trend reversal algorithms, (iv) Demonstrate that with our proposed DC-based trading strategy, which utilises  
383 our proposed trend reversal approach, profitable trading decisions can be made with reduced risk in comparison to  
384 trading strategies experimented . The first and second goals are addressed in Sections 5.1 respectively while the the  
385 remainder are addressed in Section 5.3.

### 386 5.1. Classification result

387 We measure the performance of our classification models according to accuracy, precision and recall. Table 4  
388 presents the average results over the 5 DC thresholds and over the 10 months of data, per currency pair. The total  
389 average accuracy, precision and recall across the 20 currency pairs we experimented are 0.817, 0.842 and 0.822  
390 respectively. The least average accuracy record currency pair was 0.780 (USD/SGD). The least average precision  
391 recorded per currency pair was 0.620 (EUR/CSK), however the remaining 19 average results were all above 0.820.  
392 The least average recall recorded per currency pair was 0.419 (EUR/CSK), however the remaining currency pair  
393 averages were above 0.713. These results are very important, because they will allow the GP, the next step in our  
394 proposed framework, to perform regression only on DC trends that are classified to have a DC and a corresponding  
395 OS event ( $\alpha DC$ ). Therefore, the fact that we have such high values of accuracy, precision and recall for most currency  
396 pairs will allow us to obtain better results when predicting the end of a trend. This will become evident in the next  
397 section, where the addition of the classification step has led to a much reduced regression error.

### 398 5.2. Regression result

399 Table 5 presents the average RMSE result of the regression step over the 5 DC thresholds and over the 10 months  
400 of data, per currency pair. We predict OS event length in DC trends classified as  $\alpha DC$  in the classification step. The  
401 table also presents currency pair average RMSE results of other OS event length estimation techniques, which we  
402 described with Equations 1, 2, and 3. From the table we see that our framework that uses the classification and GP  
403 steps (C+GP) consistently outperforms other trend reversal estimators in 13 of the 20 currency pairs. It also ranks  
404 second in five cases, behind Equation 3 (the predecessor of our proposed C+GP presented in Adegboye et al. (2017),

<b>Data</b>	<b>Accuracy</b>	<b>Precision</b>	<b>Recall</b>
AUD/JPY	0.851	0.867	0.839
AUD/NZD	0.805	0.827	0.817
AUD/USD	0.829	0.851	0.832
CAD/JPY	0.820	0.825	0.828
EUR/AUD	0.821	0.833	0.866
EUR/CAD	0.839	0.850	0.890
EUR/CSK	0.557	0.620	0.419
EUR/GBP	0.825	0.857	0.857
EUR/JPY	0.821	0.858	0.874
EUR/NOK	0.818	0.841	0.811
EUR/USD	0.806	0.847	0.880
GBP/AUD	0.837	0.896	0.804
GBP/CHF	0.831	0.860	0.861
GBP/USD	0.851	0.858	0.897
NZD/USD	0.848	0.862	0.874
USD/CAD	0.797	0.841	0.829
USD/JPY	0.850	0.863	0.877
USD/NOK	0.887	0.889	0.851
USD/SGD	0.780	0.820	0.816
USD/ZAR	0.877	0.869	0.713
<b>Average</b>	<b>0.817</b>	<b>0.842</b>	<b>0.822</b>

Table 4: Average accuracy, precision and recall results. 1000 datasets consisting of 5 different dynamically generated thresholds tailored to each DC dataset, 20 currency pairs, and 10 months of 10-minute interval data for each currency pair.

405 which evolved GP symbolic regression models, assuming all DC trends have a corresponding OS event). In addition,  
406 C+GP has the lowest average RMSE across all datasets, which is 18.617. This positive result confirms the strength  
407 of GP in itself to finding an equation that best represent the relationship between DC and OS event lengths. The  
408 introduction of the classification step into the GP step has been proven a successful addition, based on the average  
409 RMSE results. To support our findings, we applied Friedman’s non-parametric statistical test. The null hypothesis  
410 is that the algorithms come from the same continuous distribution. For each algorithm/equation, the table shows  
411 the average rank according to the Friedman test (first column), and the adjusted p-value of the statistical test when  
412 that equation’s average rank is compared to the average rank of the algorithm with the best rank (control algorithm)  
413 according to the Hommel post-hoc test (second column). As we can observe, our prosed approach of C+GP ranks first  
414 and statistically outperforms at the  $\alpha = 0.05$  level Equations 1 and 2. It is also worth noting that Equation 3, which as  
415 we have mentioned is the predecessor to our approach, ranks second.

416 To sup up the findings so far, we can make two important observations: (i) the addition of the classification step

417 (C+GP) to our existing algorithm that was only using regression to predict the trend reversal has significantly reduced  
418 the predictive error, and (ii) our proposed C+GP algorithm ranks first and significantly outperforms two out of the  
419 three other trend reversal equations.

420 Our interest now shifts to using this C+GP as the trend reversal estimation algorithm of a DC-based trading  
421 strategy, to investigate whether estimating trend reversal in this manner can lead to an increase trading profit margins.

Algorithms	C+GP	Equation 1	Equation 2	Equation 3
AUD/JPY	<b>15.567</b>	22.269	25.527	15.627
AUD/NZD	27.368	41.592	51.242	<b>24.332</b>
AUD/USD	<b>11.580</b>	14.060	16.095	12.814
CAD/JPY	<b>11.843</b>	27.251	39.970	18.785
EUR/AUD	21.171	<b>19.749</b>	25.728	20.569
EUR/CAD	<b>16.205</b>	24.867	23.183	17.719
EUR/CSK	<b>41.990</b>	83.845	188.608	52.949
EUR/GBP	24.173	<b>18.790</b>	31.430	22.635
EUR/JPY	<b>19.965</b>	25.204	28.162	21.117
EUR/NOK	<b>13.717</b>	22.499	27.201	13.762
EUR/USD	<b>28.260</b>	30.038	38.532	31.061
GBP/AUD	15.138	17.910	21.670	<b>14.719</b>
GBP/CHF	<b>15.961</b>	23.669	19.358	17.204
GBP/USD	<b>19.204</b>	27.778	21.223	24.889
NZD/USD	<b>10.230</b>	15.896	14.731	10.588
USD/CAD	26.934	29.315	34.654	<b>26.818</b>
USD/JPY	<b>13.704</b>	18.326	17.998	14.543
USD/NOK	7.718	10.764	14.128	<b>7.357</b>
USD/SGD	<b>26.932</b>	34.360	41.712	34.148
USD/ZAR	5.440	7.720	7.796	<b>4.796</b>
<b>Average</b>	<b>18.617</b>	25.795	34.477	20.265

Table 5: Average RMSE values for each OS length estimator algorithm. 1000 datasets consisting of 5 different dynamically generated thresholds tailored to each DC dataset, 20 currency pairs, and 10 months of 10-minute interval data for each currency pair. Best result per currency pair presented in boldface.

### 422 5.3. Trading result

#### 423 5.3.1. Comparison against DC-based and technical analysis algorithms

424 Table 7 presents currency pair summary returns of the trading strategies that we detailed in Section 4.3. We would  
425 like to draw attention of reader to cases where 0.000s are reported as return in Tables tables 7, 9 and 10; this indicates  
426 that for a given currency pair, a hold action was taken by the trading strategy in the 10 months period we experimented.

Algorithm	Average Rank	$Adjust_{pHommel}$
C+GP (c)	1.450	-
Equation 3	<b>1.850</b>	0.327
Equation 1	<b>3.000</b>	2.932E-4
Equation 2	<b>3.700</b>	1.068E-7

Table 6: Statistical test results of OS length estimation according to the non-parametric Friedman test with the Hommel post-hoc test. Significant differences at the  $\alpha = 0.05$  level are shown in boldface.

427 We can see in Table 7 that our C+GP+TS algorithm ranks first in 12 out of 17 currency pairs; in addition, there's 3  
428 pairs (AUD/JPY, CAD/JPY, USD/JPY) that no trading took place. It is also worth noting that with the exception of two  
429 currency pairs (EUR/USD, GBP/USD), in all other cases where trading took place, C+GP+TS showed positive returns  
430 over the 10-month period of our experiments. It is also worth noting that of the remaining 5 currency pairs, where  
431 C+GP+TS did not come first, a DC-based strategy was best in 4. To support our findings, we applied Friedman's  
432 non-parametric statistical test. The null hypothesis is that the algorithms come from the same continuous distribution.  
433 The result of the statistical test is presented in Table 8 and shows that C+GP+TS is ranking the highest, and that the  
434 difference in ranking is statistically significant when it is compared to all other algorithms at the 5% level.

435 In Table 9 we report the maximum return per currency pair (i.e. 10 months  $\times$  5 thresholds) of the different trading  
436 strategies compared. C+GP+TS recorded the highest average maximum return over the 17 currency pairs where  
437 trading took place. It had the maximum returns in 10 currency pairs. It can also be observed that all DC based  
438 trading strategies record higher maximum return than technical indicator based trading strategies (the only exception  
439 is EUR/AUD). In similar manner, Table 10 presents minimum return per currency pair. Results show that C+GP+TS  
440 recorded the lowest average negative return (-1.087) amongst DC- based trading strategies over the 17 currency pairs  
441 with active trading. However, amongst all trading strategies, Aroon recorded the least average negative return in 11 of  
442 the 17 currency pairs where active trading took place. Overall, with regards to minimum returns, the technical analysis  
443 indicators have fewer losses compared to the DC-based indicators. It appears that technical analysis indicators take  
444 less risks, and thus are able to return lower losses.

445 Besides trading returns, it is also important to measure the risk involve. To measure risk, we present MDD and  
446 Sharpe ratio comparison result which are our metrics for measuring risk. We did not record result for currency pairs  
447 AUD/JPY, CAD/JPY and USD/JPY, as active trading did not took place in these markets. Table 11 presents the MDD  
448 result. The best average MDD result was recorded by Aaron based trading strategy. The Friedman test presented  
449 in Table 12 confirms what we mentioned earlier, i.e. that in terms of risk, technical analysis indicators are more  
450 conservative.

451 To obtain a more holistic view of the results, we also use the Sharpe ratio, which is a well-known aggregate metric  
452 of return and risk. Figure 6 presents a chart that details the Sharpe ratio results of the trading strategies. The x-axis  
453 presents the time period covered for the relevant currency pair, and the y-axis presents average risk-adjusted return in

454 percentages. We do not present Sharpe ratio result for markets where there weren't active trading. As we can observe,  
 455 C+GP+TS is the trading strategy that records the highest number of positive Sharp ratio for a total of 28 times in  
 456 the 5 month summary chart. Meanwhile, GP+TS, MF+TS, O+TS, EMA, BOLLIN, SMA , AROON, ROC, RSI and  
 457 MACD had 11, 7, 17, 8, 3, 11, 4, 3, 12 and 4 positive Sharpe ratio results, respectively. Of the 28 positive Sharpe  
 458 ratio results, 6 where above 0.5, 24 were above 0.2 and the rest were below 0.2.<sup>1</sup> Table 13 presents the Friedman test.  
 459 It confirms our observations, and C+GP+TS ranks first and statistically outperforms all the other trading strategies at  
 460 the 5% level.

461 This is perhaps the most important result so far, as it demonstrates that when considering both returns and risk, our  
 462 proposed algorithm is able to outperform all other algorithms tested in this paper, both DC-based and also non DC-  
 463 based. It is also particularly important that C+GP+TS is able to statistically outperform seven well-known technical  
 464 analysis indicators.

### 465 5.3.2. Comparison with Buy-and-hold

466 Since C+GP+TS has been shown to be the best algorithm across all other DC and technical analysis based algo-  
 467 rithms, we will now compare it with the well-known buy-and-hold (BandH) benchmark. The reason we are doing this  
 468 comparison separately is because for BandH we do not have 10 monthly datasets, as we did with all other algorithms.  
 469 Instead, we simply buy on the first day of the first month, and sell on the last day of the tenth month.

470 Table 14 presents comparison trading result between C+GP+TS and BandH. C+GP+TS recorded positive mean  
 471 annual return in 18 of 20 markets. It outperformed BandH in 12 currency pairs. C+GP+TS's average return across  
 472 all currency pairs is 0.225% and that of BandH is -0.121%. C+GP+TS reported a variance of 0.153 and BandH's  
 473 reported a variance of 0.515. This result shows that C+GP+TS is more profitable and less risky that BandH. Finally  
 474 we performed the Kolmogorov-Smirnov statistical test to investigate whether there is statistical significance in their  
 475 results. The p-value of the test was 7.2529e-04, which confirms the statistical significance of the performance of  
 476 C+GP+TS over that of BandH. Thus, the fact that C+GP+TS is more profitable and less risky, outperforming BandH  
 477 in more markets makes it a more attractive investment strategy.

### 478 5.3.3. A sample of best GP models

479 For completeness, we present some of the equations that our symbolic regression GP evolved below, in their  
 480 equation format (and not in their tree format).  $OS_l$  is the OS length and  $DC_l$  is DC length. These four examples are  
 481 four of our best trees in terms of profitability over all our datasets.

$$OS_l = \log(a + DC_l^b) \tag{9}$$

where a= 1609.55 and b = 5.023.

---

<sup>1</sup>A ratio of 0.2-0.3 is in line with the general market. A value of 0.5 is considered a market-beating performance if achieved over a long period, a ratio of 1 or better considered superb and difficult to achieve over long periods and a negative Sharpe ratio indicates negative returns.

Trading strategies	C+GP+TS	GP+TS	M+TS	O+TS	EMA	BOLLIN	SMA	AROON	ROC	RSI	MACD
AUD/JPY	0.000	0.000	0.000	0.000	0.000	0.000	0.000	0.000	0.000	0.000	0.000
AUD/NZD	<b>0.260</b>	-0.089	-0.063	-0.012	0.002	-0.007	-0.026	-0.002	-0.447	0.056	0.005
AUD/USD	<b>0.273</b>	-0.464	-0.327	-0.132	-0.145	-0.393	-0.069	-0.025	-0.321	0.046	-0.147
CAD/JPY	0.000	0.000	0.000	0.000	0.000	0.000	0.000	0.000	0.000	0.000	0.000
EUR/AUD	<b>0.186</b>	-0.039	-0.124	0.055	0.057	-0.365	-0.127	0.002	-0.166	-0.060	-0.092
EUR/CAD	<b>0.192</b>	-0.243	-0.019	-0.151	-0.226	-0.759	-0.032	-0.068	-0.486	-0.013	-0.346
EUR/CSK	0.034	0.010	<b>0.035</b>	0.005	-0.233	-0.067	-0.164	0.000	-0.781	-0.138	-0.281
EUR/GBP	<b>0.104</b>	-0.087	-0.061	0.032	-0.135	-0.067	-0.048	-0.061	-0.367	-0.028	-0.240
EUR/JPY	<b>0.020</b>	-0.062	-0.020	-0.016	0.015	0.000	-0.027	0.000	0.000	-0.022	0.013
EUR/NOK	<b>0.351</b>	-0.043	-0.148	-0.069	-0.118	-0.232	0.149	0.003	-0.261	-0.043	-0.233
EUR/USD	-0.001	0.020	-0.105	<b>0.032</b>	-0.492	-0.366	-0.250	-0.064	-0.262	-0.106	-0.409
GBP/AUD	0.354	0.296	-0.247	<b>0.406</b>	-0.302	-0.201	-0.022	-0.061	-0.531	-0.159	-0.061
GBP/CHF	<b>0.202</b>	-0.116	-0.087	-0.028	-0.268	-0.356	0.009	-0.087	-0.653	0.035	-0.331
GBP/USD	-0.059	-0.048	-0.203	-0.047	-0.076	-0.610	-0.111	-0.045	-0.337	<b>0.008</b>	-0.361
NZD/USD	<b>0.280</b>	-0.478	-0.159	-0.174	-0.234	-0.445	-0.151	-0.025	-0.333	0.124	-0.366
USD/CAD	<b>0.044</b>	0.011	-0.224	0.022	-0.306	-0.640	-0.458	-0.016	-0.708	-0.299	-0.571
USD/JPY	0.000	0.000	0.000	0.000	0.000	0.000	0.000	0.000	0.000	0.000	0.000
USD/NOK	<b>0.461</b>	-0.021	-0.433	-0.019	-0.075	-0.592	0.069	-0.048	-0.700	-0.144	-0.154
USD/SGD	0.030	0.027	-0.023	<b>0.130</b>	-0.044	-0.122	-0.178	-0.015	-0.513	-0.057	-0.295
USD/ZAR	<b>1.762</b>	0.840	0.695	0.487	0.344	-0.573	-0.356	0.004	-0.057	0.044	0.110
Average Return	0.225	-0.024	-0.076	0.026	-0.112	-0.290	-0.090	-0.025	-0.346	-0.038	-0.188

Table 7: Average return result for trading strategies compared. 10-minute interval out-of-sample data. 20 different currency pairs and 10 calendar months each representing the physical dataset. 5 DC dataset were generated using 5 dynamically generated thresholds tailored to each DC dataset. Best result per currency pair presented in boldface.

Trading strategies	Average Rank	<i>Adjust<sub>pHommel</sub></i>
C+GP+TS (c)	4.408	-
O+TS	<b>5.338</b>	3.609E-10
RSI	<b>5.470</b>	1.654E-12
AROON	<b>5.547</b>	4.805E-14
GP+TS	<b>5.559</b>	3.488E-14
M+TS	<b>5.775</b>	1.587E-19
SMA	<b>6.032</b>	3.884E-27
EMA	<b>6.196</b>	1.336E-32
MACD	<b>6.809</b>	5.218E-58
BOLLIN	<b>7.057</b>	2.329E-70
ROC	<b>7.806</b>	3.752E-115

Table 8: Statistical test results of returns according to the non-parametric Friedman test with the Hommel post-hoc test. 10-minute interval out-of-sample date. Significant differences at the  $\alpha = 0.05$  level are shown in boldface. BOLLIN is Bollinger bandwidth indicator

Trading strategies	C+GP+TS	GP+TS	M+TS	O+TS	EMA	BOLLIN	SMA	AROON	ROC	RSI	MACD
AUD/JPY	0.000	0.000	0.000	0.000	0.000	0.000	0.000	0.000	0.000	0.000	0.000
AUD/NZD	<b>2.325</b>	1.857	1.231	1.387	0.598	0.823	1.242	0.157	0.138	0.347	0.641
AUD/USD	<b>3.551</b>	1.481	1.219	1.806	0.324	0.596	0.425	0.000	0.696	0.461	0.445
CAD/JPY	0.000	0.000	0.000	0.000	0.000	0.000	0.000	0.000	0.000	0.000	0.000
EUR/AUD	1.763	1.380	1.089	1.212	0.950	0.107	0.743	0.361	<b>1.791</b>	0.200	0.458
EUR/CAD	<b>2.119</b>	1.193	2.310	1.374	0.658	-0.117	0.537	0.067	0.059	0.299	0.764
EUR/CSK	0.424	0.449	<b>0.627</b>	0.222	0.057	0.000	0.000	0.000	-0.444	0.478	0.000
EUR/GBP	0.906	1.044	1.074	<b>1.457</b>	0.541	1.210	0.588	0.000	0.542	0.260	0.554
EUR/JPY	0.433	<b>0.557</b>	0.429	0.412	0.154	0.000	0.131	0.000	0.000	0.000	0.135
EUR/NOK	<b>2.534</b>	1.216	1.613	0.748	0.081	1.125	1.283	0.074	0.646	0.128	0.853
EUR/USD	<b>1.004</b>	0.926	0.785	0.736	0.000	0.206	0.214	0.201	0.476	0.050	0.415
GBP/AUD	2.764	<b>3.121</b>	1.247	3.252	0.255	1.136	1.112	0.017	0.262	0.938	1.413
GBP/CHF	<b>2.065</b>	1.124	0.940	1.366	0.643	0.174	0.498	0.000	0.041	0.456	0.228
GBP/USD	<b>1.577</b>	1.064	0.813	0.925	0.588	0.444	0.313	0.000	0.207	0.302	0.063
NZD/USD	3.059	1.896	<b>3.683</b>	1.647	0.489	0.406	0.486	0.000	0.982	0.779	1.017
USD/CAD	1.868	<b>2.104</b>	1.614	2.207	1.441	0.420	0.422	0.000	0.368	0.183	0.887
USD/JPY	0.000	0.000	0.000	0.000	0.000	0.000	0.000	0.000	0.000	0.000	0.000
USD/NOK	<b>3.273</b>	1.723	3.054	2.214	0.843	0.652	1.034	0.000	0.026	0.069	0.730
USD/SGD	<b>1.336</b>	1.213	0.526	1.678	0.460	0.805	0.000	0.000	0.247	0.330	0.513
USD/ZAR	<b>7.129</b>	5.045	4.507	3.601	2.603	0.935	0.743	0.038	2.421	0.684	2.323
Average Maximum	1.907	1.370	1.338	1.312	0.534	0.446	0.489	0.046	0.423	0.298	0.572

Table 9: % Maximum return result for trading strategies compared. 10-minute interval out-of-sample data. 20 different currency pairs and 10 calendar months each representing the physical dataset. 5 DC dataset were generated using 5 dynamically generated thresholds tailored to each DC dataset. Best result per currency pair is shown in boldface. BOLLIN is Bollinger bandwidth indicator

$$OS_l = \log((DC_l \times a)^b) \quad (10)$$

where a= 4.117 and b = 5.764.

$$OS_l = \cos(a \times \cos(DC_l)) + \frac{b}{\exp(\cos(DC_l))} \quad (11)$$

where a = 292.160 and b= 4.569

$$OS_l = \exp(\exp(\sin(\sin(DC_l)))) + (a \times (b + \log(DC_l))) \quad (12)$$

where a = 1.750 and b = 1.957.



Trading strategies	C+GP+TS	GP+TS	M+TS	O+TS	EMA	BOLLIN	SMA	AROON	ROC	RSI	MACD
AUD/JPY	0.000	0.000	0.000	0.000	0.000	0.000	0.000	0.000	0.000	0.000	0.000
AUD/NZD	-1.189	-1.559	-1.048	-1.578	-0.482	-0.620	-0.507	<b>-0.120</b>	-0.836	-0.170	-1.040
AUD/USD	-1.918	-3.646	-3.240	-1.143	-1.022	-1.375	-0.578	<b>-0.136</b>	-1.265	-1.037	-1.170
CAD/JPY	0.000	0.000	0.000	0.000	0.000	0.000	0.000	0.000	0.000	0.000	0.000
EUR/AUD	-0.632	-2.024	-1.092	-2.249	-0.605	-1.059	-0.695	<b>-0.209</b>	-1.013	-0.560	-0.722
EUR/CAD	-1.299	-1.801	-1.446	-1.727	-1.285	-1.717	-0.741	-0.477	-1.123	<b>-0.298</b>	-2.068
EUR/CSK	-0.168	-0.202	-0.197	-0.037	-0.670	-0.200	-0.315	<b>0.000</b>	-1.586	-0.380	-0.626
EUR/GBP	-0.619	-1.206	-0.743	-0.970	-0.503	-1.245	-0.648	-0.454	-0.855	<b>-0.376</b>	-0.992
EUR/JPY	0.000	-1.344	-0.658	-1.185	<b>0.000</b>	0.000	-0.397	0.000	0.000	-0.222	<b>0.000</b>
EUR/NOK	-0.863	-1.490	-1.743	-1.404	-0.499	-1.282	-0.650	-0.043	-1.177	<b>-0.411</b>	-1.182
EUR/USD	-1.189	-0.744	-1.032	-0.563	-1.181	-1.032	-1.229	<b>-0.326</b>	-0.882	-0.940	-1.102
GBP/AUD	-1.506	-2.736	-2.368	-1.800	-1.250	-1.610	-0.837	<b>-0.361</b>	-2.061	-1.928	-0.755
GBP/CHF	-0.811	-1.542	-1.274	-0.969	-1.546	-1.072	-0.469	-0.359	-2.566	<b>-0.101</b>	-0.994
GBP/USD	-0.938	-2.396	-1.009	-2.665	-0.658	-1.293	-0.588	-0.390	-1.052	<b>-0.200</b>	-0.774
NZD/USD	-1.758	-2.556	-1.631	-2.612	-1.659	-1.952	-0.995	-0.086	-1.265	<b>0.000</b>	-1.028
USD/CAD	-1.870	-2.625	-3.111	-2.758	-2.010	-1.974	-2.351	<b>-0.156</b>	-1.698	-2.092	-2.501
USD/JPY	0.000	0.000	0.000	0.000	0.000	0.000	0.000	0.000	0.000	0.000	0.000
USD/NOK	-3.141	-1.644	-5.282	-1.374	-1.136	-2.051	-0.851	<b>-0.343</b>	-1.534	-0.935	-1.669
USD/SGD	-0.724	-0.647	-0.847	-0.493	-0.567	-0.861	-0.528	<b>-0.146</b>	-1.462	-0.544	-0.762
USD/ZAR	-3.105	-4.979	-3.339	-5.292	-2.164	-2.201	-1.204	<b>0.000</b>	-3.504	-0.702	-2.679
Average Minimum	-1.087	-1.657	-1.503	-1.441	-0.862	-1.077	-0.679	-0.180	-1.194	-0.545	-1.003

Table 10: % Minimum return result for trading strategies compared. 10-minute interval out-of-sample data. 20 different currency pairs and 10 calendar months each representing the physical dataset. 5 DC dataset were generated using 5 dynamically generated thresholds tailored to each DC dataset. Best result per currency pair shown in boldface. BOLLIN is Bollinger bandwidth indicator

482 As we can observe, most equations have different structures. The first two are logarithmic equations, whereas the  
483 third has both the cosine and the exponential functions, and the fourth equation has exponential, sine and logarithmic  
484 functions. This is particularly interesting and important, because it demonstrates that the relationship between the  
485 DC and OS lengths can be non-linear and also dependent on the dataset. Thus our work of using classification and  
486 regression to predict the OS length has allowed us to uncover this relationship for each dataset and increase the  
487 profitability of the trading strategies.

#### 488 5.3.4. Computational times

489 Table 15 presents the average computational times for all algorithms. We should note that because MF+TS,  
490 O+TS, EMA, BOLLIN, SMA, AROON, ROC, RSI and MACD and BandH are deterministic algorithms and don't  
491 have the extra step of training models, their execution is faster taking from around 3 seconds to 30 seconds. C+GP+TS  
492 and GP+TS are non-deterministic algorithms, thus their execution times vary between around 5 and 70 minutes. The

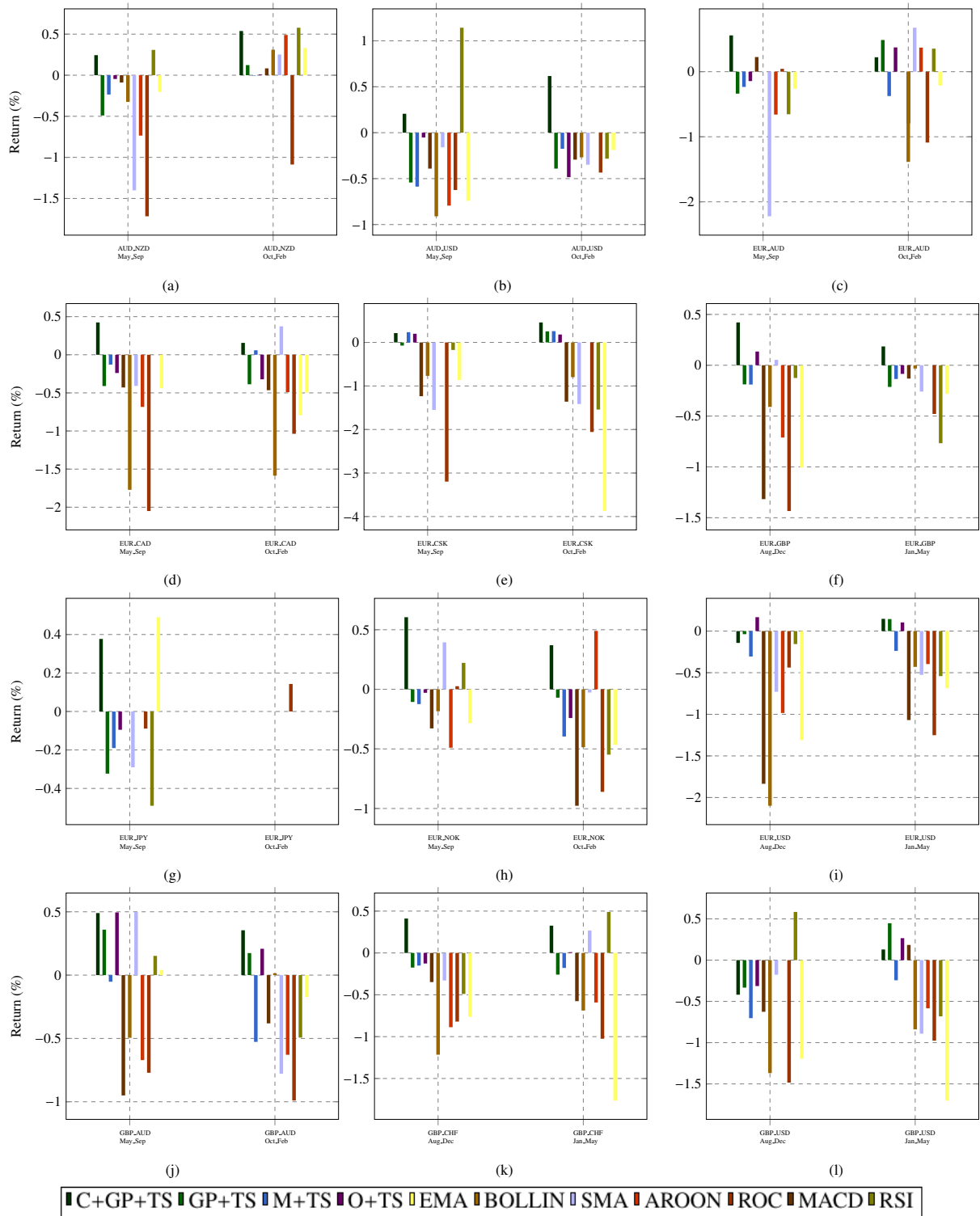
Trading strategies	C+GP+TS	GP+TS	M+TS	O+TS	EMA	BOLLIN	SMA	AROON	ROC	RSI	MACD
AUD/NZD	0.123	0.151	0.159	0.206	0.170	0.368	0.286	<b>0.018</b>	0.681	0.071	0.159
AUD/USD	0.160	0.312	0.148	0.275	0.118	0.634	0.228	<b>0.025</b>	0.622	0.162	0.170
EUR/AUD	0.106	0.155	0.077	0.206	0.120	0.496	0.380	<b>0.041</b>	0.508	0.104	0.173
EUR/CAD	0.135	0.258	0.203	0.308	0.123	0.823	0.172	0.089	<b>0.748</b>	0.080	0.148
EUR/CSK	0.006	0.008	0.013	0.002	0.036	0.074	0.166	<b>0.003</b>	0.783	0.186	0.039
EUR/GBP	0.100	0.078	0.137	0.086	0.242	0.372	0.204	<b>0.064</b>	0.532	0.072	0.196
EUR/JPY	0.011	0.038	0.008	0.052	0.004	0.000	0.040	0.000	0.000	0.022	0.001
EUR/NOK	0.133	0.148	0.256	0.152	0.114	0.469	0.186	<b>0.004</b>	0.688	0.090	0.101
EUR/USD	0.155	<b>0.069</b>	0.126	0.083	0.224	0.495	0.299	0.095	0.416	0.191	0.223
GBP/AUD	0.191	0.239	0.201	0.177	0.208	0.731	0.273	<b>0.081</b>	1.030	0.283	0.216
GBP/CHF	0.096	0.106	0.049	0.191	0.163	0.525	0.281	0.087	0.780	<b>0.016</b>	0.200
GBP/USD	0.132	0.180	0.122	0.162	0.122	0.842	0.340	<b>0.077</b>	0.508	0.112	0.270
NZD/USD	0.289	0.324	0.266	0.404	0.270	0.861	0.385	<b>0.026</b>	0.698	0.000	0.263
USD/CAD	0.168	0.162	0.340	0.239	0.323	0.898	0.609	<b>0.024</b>	0.906	0.333	0.167
USD/NOK	0.141	0.175	0.569	0.172	0.235	1.051	0.245	<b>0.054</b>	0.928	0.173	0.099
USD/SGD	0.077	0.074	0.069	0.036	0.127	0.316	0.267	<b>0.015</b>	0.590	0.152	0.079
USD/ZAR	0.117	0.145	0.281	0.331	0.357	1.476	0.628	<b>0.000</b>	1.069	0.149	0.709
Average MDD	0.107	0.131	0.151	0.154	0.148	0.522	0.249	<b>0.035</b>	0.574	0.110	0.161

Table 11: %Average maximum drawdown results for 10-minute interval out-of-sample data. 20 different currency pairs and 10 calendar months each representing the physical dataset. 5 DC dataset were generated using 5 dynamically generated thresholds tailored to each DC dataset. Best result per currency pair shown in boldface.

Trading strategies	Average Rank	<i>Adjust<sub>pHommel</sub></i>
BOLLIN (c)	2.162	-
AROON	<b>3.291</b>	2.635E-14
RSI	<b>5.639</b>	2.952E-121
C+GP+TS	<b>5.962</b>	2.769E144
O+TS	<b>5.338</b>	1.693E-146
GP+TS	<b>6.171</b>	3.106E-160
M+TS	<b>6.181</b>	5.994E-161
EMA	<b>6.771</b>	3.802E-211
MACD	<b>7.099</b>	4.514E-242
SMA	<b>7.342</b>	2.611E-266
ROC	<b>9.386</b>	0.0

Table 12: : Statistical test results of maximum drawdown of DC based trading strategies according to the non-parametric Friedman test with the Hommel post-hoc test. 10-minute interval out-of-sample data. Significant differences at the  $\alpha = 0.05$  level are shown in boldface.

493 higher computation times for C+GP+TS was expected. This is because we configured AutoWeka to run for 60 minutes  
494 in order to search for the most suitable classifier and optimise its hyperparameters which we also mentioned in Section



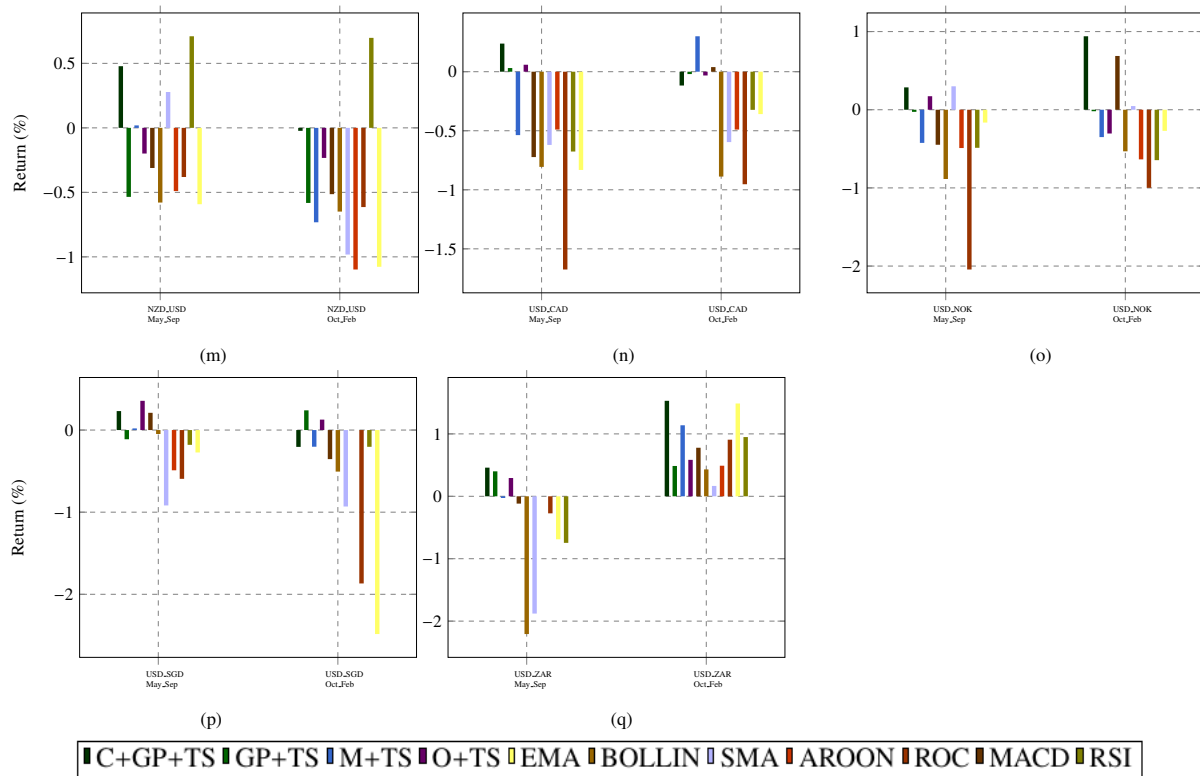


Figure 6: Average Sharpe ratio for all currency pairs.

Trading strategies	Average Rank	$Adjust_{pHommel}$
C+GP+TS (c)	2.399	-
O+TS	<b>3.971</b>	0.047
GP+TS	<b>5.000</b>	0.002
M+TS	<b>5.314</b>	7.112E-4
RSI	<b>5.600</b>	2.173E-4
SMA	<b>6.229</b>	6.860E-6
EMA	<b>6.357</b>	3.600E6
AROON	<b>6.600</b>	8.217E-7
MACD	<b>7.529</b>	7.906E-10
BOLLIN	<b>8.000</b>	1.462E-11
ROC	<b>9.000</b>	8.457E-16

Table 13: Statistical test results of the Sharpe ratio results according to the non-parametric Friedman test with the Hommel post-hoc test. 10-minute interval out-of-sample date. Significant differences at the  $\alpha = 0.05$  level

495 4.3.<sup>2</sup> Auto-WEKA can be executed in both single-threaded and multi-threaded modes. We have chosen to perform  
 496 our experiments using single threaded mode due to limited hardware resources. The minimum execution time for

<sup>2</sup>The time taken in the classification phase of C+GP+TS went above the allotted time of 60 minutes due to CPU time slice as other processes were running on the hardware simultaneously.

Trading strategies	C+GP+TS	Buy-and-hold
AUD/JPY	<b>0.000</b>	-6.278
AUD/NZD	<b>0.260</b>	-0.516
AUD/USD	<b>0.273</b>	-5.728
CAD/JPY	<b>0.000</b>	-4.109
EUR/AUD	<b>0.186</b>	-2.672
EUR/CAD	0.192	<b>18.555</b>
EUR/CSK	0.034	<b>7.770</b>
EUR/GBP	<b>0.104</b>	-0.292
EUR/JPY	<b>0.020</b>	-6.211
EUR/NOK	0.351	<b>2.046</b>
EUR/USD	-0.001	<b>8.801</b>
GBP/AUD	0.354	<b>3.936</b>
GBP/CHF	<b>0.202</b>	-2.395
GBP/USD	-0.059	<b>8.464</b>
NZD/USD	<b>0.280</b>	-6.443
USD/CAD	0.044	<b>2.345</b>
USD/JPY	<b>0.000</b>	-9.430
USD/NOK	<b>0.461</b>	-6.102
USD/SGD	0.030	<b>0.207</b>
USD/ZAR	<b>1.762</b>	-4.505
Mean	<b>0.225</b>	-0.128

Table 14: % Mean trading result of C+GP+TS vs Buy-and-hold trading strategies per currency pair. 10-minute interval out-of-sample data. Results show RMSE value. They are averaged over 5 different dynamically generated thresholds tailored to each DC dataset and 20 currency pairs.

Trading strategies	C+GP+TS	GP+TS	M+TS	O+TS	EMA	BOLLIN	SMA	AROON	ROC	RSI	MACD
Classification	~ 65 mins	-	-	-	-	-	-	-	-	-	-
Regression	~ 5.45 mins	~ 6.2 mins	~ 30 secs	~ 20 secs	-	-	-	-	-	-	-
Trading	~ 3 sec	~ 3 sec	~ 3 sec	~ 3 sec	~ 3 sec	~ 3 sec	~ 3 sec	~ 3 sec	~ 3 sec	~ 3 sec	~ 3 sec

Table 15: Average computational times per run for C+GP+TS, GP+TS, M+TS, O+TS, EMA, BOLLIN, SMA, AROON, ROC, RSI and MACD. BH is deterministic algorithms and only take around 1 second to execute.

497 Auto-WEKA is 1 minute. With the right amount of hardware resources and executing Auto-WEKA in multithreaded  
498 mode, this huge amount of time spent on searching for suitable classifier can be reduced significantly. The regression  
499 task of C+GP+TS took only 5.45 minutes on average, which is comparable to its predecessor's 6.2 minutes. Since GP  
500 is involved, it is not surprising that additional time is needed to evolve a suitable symbolic regression model. MF+TS  
501 and OS+TS on the other hand make is a simple calculation once the DC event length is determined, hence the speed  
502 in regression phase. To further improve computation time taken by the evolutionary algorithm (GP), we can also

503 parallelise the training which can reduce the time taken by up to 21 folds Brookhouse et al. (2014). Lastly, the trading  
504 task has the same duration across all algorithms: less than 3 seconds.

505 It is also important to note that for trading we would normally perform the learning processes on the training  
506 data off-line, then apply the best model to the test data. Thus, the fact that classification and regression last around  
507 70 minutes is not a problem, as for the actual trading we would simply be applying the trading model, and thus  
508 its execution would be on par with all other algorithms' execution time, including the technical analysis indicators.  
509 Finally given the significant improvements that we have observed in terms of increase in returns and reduction in risk,  
510 this slower execution time in this experimentaion scenario is justified.

#### 511 5.4. Summary

512 Based on our experimental results, we can reach the following conclusions.

513 *Using classification algorithms and GP for symbolic regression is an effective way of predicting the trend reversal*  
514 *in DC summaries.* As we observed in Tables 4 - 6, the very positive classification results have led to significant  
515 reduction in RMSE, ranking our proposed C+GP first against all other DC-based trend reversal algorithms.

516 *Utilising the above trend reversal algorithm as part of a trading strategy can lead to profitable results.* In fact,  
517 C+GP+TS significantly outperformed all other trading strategies in a variety of metrics, such as mean and maximum  
518 returns.

519 *Our proposed trading strategy is one of the least risky strategies.* As we saw from both MDD and Sharpe ratio  
520 results, C+GP+TS is a risk aversive strategy even though it prioritised market profit over capital preservation and this  
521 is confirmed in Sharpe ratio results where it outperformed other algorithms. The above thus lead us to conclude that  
522 C+GP+TS is a trading strategy with very low risk when compared to all other strategies presented in this work.

523 *There is no generalised formula for predicting trend reversal in DC-based summaries.* This is perhaps the most im-  
524 portant finding of our work. This is because it demonstrates that each dataset can have its own unique characteristics,  
525 and predicting trend reversal requires tailored solutions and not equations that are applied to all trends, irrespectively  
526 of their characteristics.

## 527 6. Conclusion

528 To conclude, this paper presented a new framework, where we used different machine learning algorithms for clas-  
529 sification and regression in DC-based summaries, to predict end of trend. This then enabled us to develop profitable  
530 and low-risk trading strategies, which were able to outperform six benchmarks, including other DC-based trading  
531 strategies, technical analysis, and buy and hold. It is important to note here that we run extensive experiments over  
532 a total of 1,000 datasets from 20 different Forex currency pairs. This thus leads us to believe that our results are not  
533 only significant, but also widely applicable.

534 Future work will focus on combining multiple DC thresholds under a single trading strategy. As we have ex-  
535 plained, each DC threshold creates a different summary. In our current work, we experimented with 5 different

536 thresholds and presented their average results. We believe that it would be interesting to combine the ‘knowledge’  
537 of multiple thresholds under an optimisation algorithm, and investigate how/if the trading strategies’ profitability can  
538 further increase. Other research directions could also be to create a tailored classification algorithm (instead of using  
539 Auto-Weka’s out-of-the-box algorithms) and further improve our GP algorithm, to reduce the error of predicting end  
540 of trend even more, and thus lead to more profitable trading strategies.

541

542 **Project code:** The source code for this project can be found in a GitHub repository, at the following address:

543 <https://github.com/adesolaadegboye/SymbolicRegression>

## 544 **References**

## 545 **References**

- 546 Abu-Mostafa, Y.S., Atiya, A.F., 1996. Introduction to financial forecasting. *Applied intelligence* 6, 205–213.
- 547 Adegboye, A., Kampouridis, M., Johnson, C.G., 2017. Regression genetic programming for estimating trend end in foreign exchange market, in:  
548 *Computational Intelligence (SSCI), 2017 IEEE Symposium Series on, IEEE*. pp. 1–8.
- 549 Aloud, M.E., 2016. Profitability of directional change based trading strategies: The case of Saudi stock market. *International Journal of Economics  
550 and Financial Issues* 6.
- 551 Azzini, A., da Costa Pereira, C., Tettamanzi, A.G., 2010. Modeling turning points in financial markets with soft computing techniques, in: *Natural  
552 Computing in Computational Finance*. Springer, pp. 147–167.
- 553 Birattari, M., Yuan, Z., Balaprakash, P., Stützle, T., 2010. F-race and iterated f-race: An overview, in: *Experimental methods for the analysis of  
554 optimization algorithms*. Springer, pp. 311–336.
- 555 Brabazon, A., Kampouridis, M., O’Neill, M., 2020. Applications of genetic programming to finance and economics: past, present, future. *Genetic  
556 Programming and Evolvable Machines*. 21, 33–53.
- 557 Brookhouse, J., Otero, F.E., Kampouridis, M., 2014. Working with opencl to speed up a genetic programming financial forecasting algorithm:  
558 initial results, in: *Proceedings of the Companion Publication of the 2014 Annual Conference on Genetic and Evolutionary Computation*, pp.  
559 1117–1124.
- 560 Cavalcante, R.C., Brasileiro, R.C., Souza, V.L., Nobrega, J.P., Oliveira, A.L., 2016. Computational intelligence and financial markets: A survey  
561 and future directions. *Expert Systems with Applications* 55, 194–211.
- 562 Chen, T.I., Chen, F.y., 2016. An intelligent pattern recognition model for supporting investment decisions in stock market. *Information Sciences  
563* 346, 261–274.
- 564 Chung, F.L., Fu, T.C., Luk, R., Ng, V., 2001. Flexible time series pattern matching based on perceptually important points. *International Joint  
565 Conference on Artificial Intelligence Workshop on Learning from Temporal and Spatial Data* , 1–7.
- 566 Frank, E., Hall, M.A., Witten, I.H., 2016. *The WEKA workbench: online appendix for Data mining: practical machine learning tools and  
567 techniques*. Morgan Kaufmann, Fourth edition.
- 568 Glattfelder, J., Dupuis, A., Olsen, R., 2011. Patterns in high-frequency FX data: discovery of 12 empirical scaling laws. *Quantitative Finance* 11,  
569 599–614.
- 570 Guillaume, D.M., Dacorogna, M.M., Davé, R.R., Müller, U.A., Olsen, R.B., Pictet, O.V., 1997. From the bird’s eye to the microscope: A survey  
571 of new stylized facts of the intra-daily foreign exchange markets. *Finance and stochastics* 1, 95–129.
- 572 Kampouridis, M., Otero, F.E., 2017. Evolving trading strategies using directional changes. *Expert Systems with Applications* 73, 145–160.
- 573 Lin, T., Guo, T., Aberer, K., 2017. Hybrid neural networks for learning the trend in time series, in: *Proceedings of the twenty-sixth international  
574 joint conference on artificial intelligence*, pp. 2273–2279.

575 López-Ibáñez, M., Dubois-Lacoste, J., Stützle, T., Birattari, M., 2011. The irace package, iterated race for automatic algorithm configuration.  
576 Technical Report. Citeseer.

577 Özorhan, M.O., Toroslu, İ.H., Şehitoğlu, O.T., 2018. Short-term trend prediction in financial time series data. *Knowledge and Information Systems*  
578 , 1–33.

579 Poli, R., Langdon, W.B., McPhee, N.F., Koza, J.R., 2008. A field guide to genetic programming. Lulu. com.

580 Samanta, S., Pratama, M., Sundaram, S., Srikanth, N., . A dual network solution (dns) for lag-free time series forecasting .

581 Thornton, C., Hutter, F., Hoos, H.H., Leyton-Brown, K., 2013. Auto-weka: Combined selection and hyperparameter optimization of classification  
582 algorithms, in: *Proceedings of the 19th ACM SIGKDD international conference on Knowledge discovery and data mining*, ACM. pp. 847–855.

583 Tsang, E., 2010. Directional changes, definitions. Working Paper WP050-10 Centre for Computational Finance and Economic Agents (CCFEA),  
584 University of Essex Revised 1, Tech. Rep. .

585 Tsang, E.P., Tao, R., Serguieva, A., Ma, S., 2017. Profiling high-frequency equity price movements in directional changes. *Quantitative finance*  
586 17, 217–225.

587 Wan, Y., Gong, X., Si, Y.W., 2016. Effect of segmentation on financial time series pattern matching. *Applied Soft Computing* 38, 346–359.

588 Yin, J., Si, Y.W., Gong, Z., 2011. Financial time series segmentation based on turning points, in: *Proceedings 2011 International Conference on*  
589 *System Science and Engineering*, IEEE. pp. 394–399.